Clinical study

Investigation of the effect of anticoagulant usage in the flow diverter stent treatment of the patient-specific cerebral aneurysm using the Lagrangian coherent structures

Muhammed Furkan Tercanlı [a], Ali Bahadır Olcay [b,*], Onur Mutlu [c], Cem Bilgin [d], Bahattin Hakyemez [e]

[a] BSH Home Appliances, BSH Cad., 59501, Tekirdag, Turkey
[b] Yeditepe University, Faculty of Engineering, Department of Mechanical Engineering, Kayisdagi Cad., 34755 Istanbul, Turkey
[c] Biomedical Research Center, Qatar University, Doha P.O. Box 2713, Qatar
[d] University of Health Sciences, Bursa Yuksek Ihtisas Training and Research Hospital, Department of Radiology, Yildirim, Bursa 16310, Turkey
[e] Uludag University School of Medicine, Department of Radiology, Gorukle, Bursa 16059, Turkey

A R T I C L E   I N F O

A B S T R A C T

Anticoagulants are prescribed to the flow diverter treated patients to diminish the risk of embolism in the arteries. In the present study, digital subtraction angiography images of a 49-year-old female patient with a left paraophthalmic aneurysm were used to build a numerical model to investigate the effect of an anti-coagulant on hemodynamics at the aneurysm site. The Carreau-Yasuda viscosity model was utilized to define blood viscosity, and the coefficients of the viscosity model were updated based on the usage of warfarin. The five-cardiac cycle-long numerical simulations were performed, and Lagrangian coherent structures, hyperbolic time, and fluid particle analyses were also employed in the numerical models. These analyses allowed us to evaluate the formation of stagnated regions, recirculation zones, and the number of jailed particles inside the aneurysm sac following a flow diverter placement. It is realized that anticoagulant use caused blood to be less viscous, yielding a substantial amount of incoming blood flow to enter the aneurysm sac. Only 12% of the nearly 25,000 fluid particles seeded from the artery inlet have stayed inside the sac. Furthermore, the deviation between warfarin added blood and normal blood flow becomes more extensive, with every heartbeat undermining the effectiveness of patient-specific CFD models when the use of anticoagulants is overlooked in the viscosity models.

© 2021 Elsevier Ltd. All rights reserved.

1. Introduction

Antithrombotic drugs usage in clinics is very common to support the circulation system and eliminate possible embolism in the arteries. While antithrombotic drugs include antiplatelets and anticoagulants, antiplatelets inhibit platelet aggregation, whereas anticoagulants prevent the formation of fibrin monomers. Antithrombotics, especially anticoagulants, have a very narrow safety margin and are associated with aneurysm rupture and spontaneous intracranial hemorrhage [1,2]. Furthermore, anticoagulants are used in the perioperative and early postoperative period, while antiplatelets are preferred for the long-term prevention of in-stent thrombosis [3,4]. However, there are multiple comorbidities where anticoagulants are the standard of care, such as atrial fibrillation, prosthetic heart valve surgery, pulmonary embolism, and deep vein thrombosis [5,6]. Given the high prevalence of these comorbidities, understanding the relationship between anticoagulant therapy and flow diversion outcome is imperative to avoid unnecessary interventions.

Flow diverter implants, as an example, have thrombogenic potential, and presently, thromboembolic complications could not be entirely prevented despite the recent advances in flow diverter technology and routine use of antithrombotics [7]. For this reason, both drugs are still indispensable in peri- and postoperative patient management. Even though these drugs' safety profile and efficacy have been well investigated in the literature, neuro-interventionalists have commonly omitted the effect of antithrombotics on aneurysm occlusion. A potent anticoagulant may significantly reduce blood viscosity and thus can increase the intra-aneurysmal blood flow. These changes in blood may jeopardize the aneurysm occlusion; therefore, selecting an ideal anticoagulant can prevent thromboembolic complications while not reversing the effects of flow diverters.

* Corresponding author.
  E-mail address: bahadir.olcay@yeditepe.edu.tr (A.B. Olcay).

All the patient-specific numerical studies related to flow diversion in the literature overlook the viscosity change of blood by neglecting the anticoagulant effect. This can significantly enlarge the gap between clinical findings and numerical model results. Therefore, this study investigates the effect of warfarin being an anticoagulant on the outcome of flow diverter-treated patients. Warfarin is a potent anticoagulant that inhibits vitamin K epoxide reductase, limiting the production of vitamin K-dependent clotting factors. It thus prevents the formation of a thrombus [5,6]. Digital subtraction angiography (DSA) images of a 49-year-old female patient with a left paraophthalmic aneurysm were used to build a computational fluid dynamics (CFD) model to investigate the effect of warfarin on hemodynamics at the aneurysm site in the present work. Furthermore, Lagrangian coherent structures analysis was also employed in the CFD models to identify the stagnated regions and number of escaped and jailed fluid particles inside the aneurysm sac.

2. Materials and methods

A 49-year-old patient with a dizziness complaint arrived in the hospital. After a careful examination, an aneurysm was identified in the patient's left internal carotid artery (LICA), as seen in Fig. 1 (A). Then, a 4-mm diameter Surpass brand FD with a 72 wire was implanted into the patient's aneurysm site in the clinic to divert the main flow from the aneurysm sac to the parent artery. Fig. 1(B) shows the aneurysm site and reduced height of the aneurysm, implying that the FD stent successfully worked at the aneurysm neck and caused a nearly 27% decrease in the height of the aneurysm at the 4th-month control.

Although flow diverter treated patients are generally prescribed with two antiplatelet agents (typically aspirin plus clopidogrel/pra surgrel/ticagrelor), the long-term effects of anticoagulants on flow diversion are still unknown [9]. Therefore, we aimed to address how anticoagulant effects on blood viscosity can affect the flow diverter outcome. While warfarin may not be considered as a first-choice anticoagulant in the flow diverter treatment, warfarin data were used in the present study because of two main reasons. First, its effects on blood viscosity were previously studied in real blood samples. Secondly, it is a highly potent anticoagulant that is used in cases who experience refractory thromboembolic events under long-term anticoagulant therapy. Although warfarin is commonly employed in various comorbidities such as atrial fibrillation, deep vein thrombosis, pulmonary embolus [10,11], there is no study investigating the effects of long-term warfarin use after flow diverter deployment.
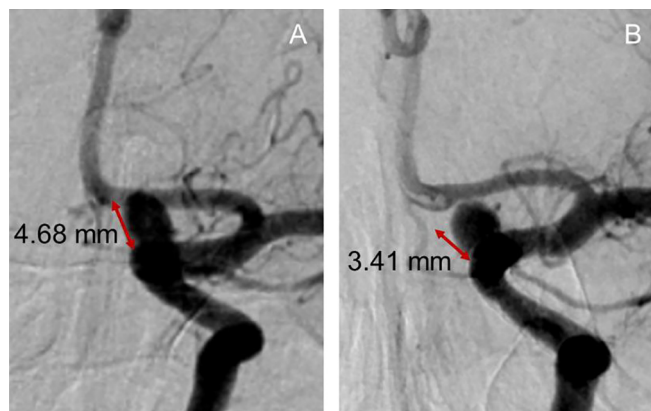

Fig. 1. DSA images of the aneurysm site: before the FD placement (A); four months after the FD deployment (B).

Blood viscosity varying with warfarin also depends on many other parameters such as hematocrit, electrolytes, solutes, red blood cells, white blood cells, and blood proteins (fibrinogen, albumin, globulin etc.). Although those parameters can affect blood viscosity, they are part of the blood viscosity value for the patient. Since whole blood viscosity (WBV) measurements were obtained by collecting blood samples from people with warfarin [8], the values provided in the study [8] have a high potential to reflect the effects of all these parameters into the blood viscosity values. On the other hand, anticoagulation is not the component of blood that can be prescribed to the patient during flow diverter treatment to prevent clotting formation on stent surfaces. Therefore, WBV with warfarin measurements were employed in a numerical model to identify the effect of anticoagulation in blood flow inside the aneurysm sac once a flow diverter stent is implanted into the patient's aneurysm neck.

In clinics, patients are generally required to use anticoagulants starting from several days before an FD placement into their aneurysm neck to the months after the treatment. It is known that the use of anticoagulants causes blood to be thinner (i.e., less viscous). Therefore, the effect of anticoagulants on blood viscosity should be taken into consideration in hemodynamics analysis to correctly mimic the blood flow in the artery since the use of anticoagulants directly affects the blood's viscosity property. Meanwhile, blood is defined as a non-Newtonian fluid with the Carreau-Yasuda viscosity model [12] given in equation (1) to capture its shear-thinning behavior in the present study. Here, μ, μ_∞, and μ_0 are viscosity, viscosity at high shear rate and viscosity at low shear rate, respectively while $\dot{\gamma}$ represents rate of deformation tensor and λ, p and n are constants. The new coefficients and constants in the the Carreau-Yasuda viscosity model were obtained from the shear rate versus blood viscosity values with warfarin [8] using the curve fitting tool of MATLAB (MathWorks, Natick, Massachusetts, USA). Then, the volumetric flow rate given according to the patient's age and gender information was selected as 297 ml/min [13]. The mean velocity value was obtained using the volumetric flow rate equation by considering the patient's vessel inlet diameter. Although this velocity value was used for normal blood flow, the Poiseuille law equation was used to find the average velocity value of blood with warfarin case by assuming the blood to be Newtonian fluid. The pressure difference between two very close points in the vessel was accepted as constant, and the Poiseuille Law equations were equalized for both normal and blood with warfarin cases. The mean velocity value for blood with warfarin was used to obtain the Womersley velocity profile, and the patient's blood velocity profile was determined for blood with warfarin case. Outlet pressure values were determined to be 115 mmHg based on the patient's arterial pressure. The flow regime was assumed to be laminar inside the computational domain since the Reynolds number of the flow stayed below the critical Reynolds number.

$$\mu = \mu_\infty + (\mu_0 - \mu_\infty)\left[1 + \left(\lambda\dot{\gamma}\right)^p\right]^{(n-1)/p} \tag{1}$$

Fig. 2 shows how the viscosity of blood varies with and without warfarin. It is noticed that when the shear rate is over 200 1/s, blood viscosity with warfarin is nearly 24% of the blood without warfarin, implying that blood can flow with much less resistance at those shear rates. Besides, blood density and molar mass were adjusted as 1060 kg/m^3 and 64.458 g/mol, respectively [14].

The computational fluid dynamics model was prepared for the one inlet and five outlets aneurysm carrying the parent artery, as shown in Fig. 3(A). FD stent placed into the aneurysm neck of the patient was modeled as a porous medium [15,16], as illustrated in Fig. 3(A). Permeability, porosity, and internal resistance loss coefficient values for the porous medium were calculated to be
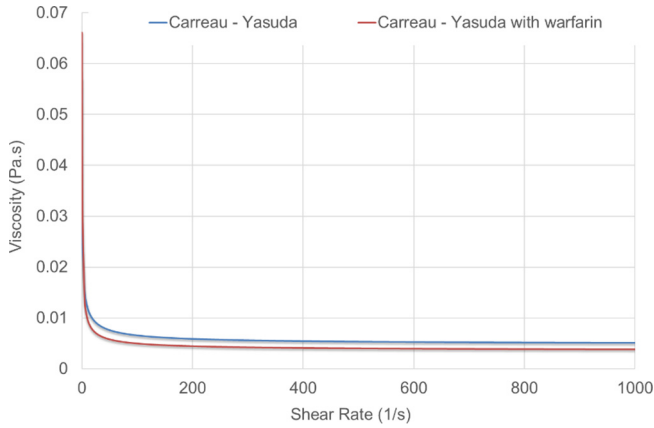
Fig. 2. Variation of blood viscosity versus shear rate for Carreau – Yasuda viscosity model with and without warfarin cases.

3.88225E-10, 0.7255, and 46804, respectively [17,18]. Besides, the porous medium thickness was set to the Surpass FD stent wire diameter of 0.032 mm. Nearly 2.5 million tetrahedral elements were placed into the CFD model, and a total of 4 s (i.e., five cardiac cycles) long simulations were carried out with ANSYS 18.2 CFX (ANSYS, Inc. Canonsburg, Pennsylvania, USA). The timestep size was set to 0.001 s, yielding a total of 4000 runs [16].

After CFD simulations are completed, velocity and corresponding location data on the curve plane, as shown in Fig. 3(B, C), were exported to be processed further for Lagrangian analyses [19–25]. The Lagrangian approach concerned with the identity of individual fluid particles keeps track of the changing velocity of individual particles as they move through the flow [26]. The computation of the finite-time Lyapunov exponent (FTLE) field is one of the most common approaches for observing Lagrangian coherent structure

(LCS). The Lyapunov exponent measures a fluid particle's future behavior sensitivity to its initial position in the flow field [26], while The FTLE field's spatial distribution can be utilized to identify prominent flow characteristics [27,28]. Besides, the FTLE field is a scalar quantity map computed at each point in a computational region. It measures the maximal separation ratio between neighboring particle orbits near each location, the average of the maximal expansion rate for a pair of particles in motion [25,29].

FTLE analyzes have recently been used to investigate vortex structures, stagnation regions, and fluid residence times in biological flows. The vortex structures formed by the movement of aortic valves of different stiffness, the flow regions separated by these structures, and the stagnation areas between the aortic valve and the wall can be determined by FTLE analysis [23,24,30]. Different flow regions in the aneurysm sac with and without stent implantation can be detected by FTLE analysis [21,22,31–34]. The time evolution of different fluid flow regions within the aneurysm can also be identified using hyperbolic time analysis [16,18]. The effectiveness of flow diverter stents can be measured using particle FTLE analysis to calculate the residence duration and density of flow particles entering the stented aneurysm [18].

In this study, FTLE fields were calculated by using the velocity results and location information obtained from a plane passing over near the centerline of the combined aneurysm and artery geometry. The particle movements in the computational domain were examined using the particle residence time (PRT) method to interpret LCS analysis results in more detail. Briefly, PRT is a discrete approach used to calculate residence time using particle orbit data. In this approach, massless particles are added into the boundary used in the flow analysis, and these particles are allowed to advance with fluid velocity magnitudes at their locations. PRT measures the amount of time it takes for particles to exit the pre-defined region and reach the time-varying starting location of the released particle. The positions of these particles are determined using the directions of the velocity vectors obtained by
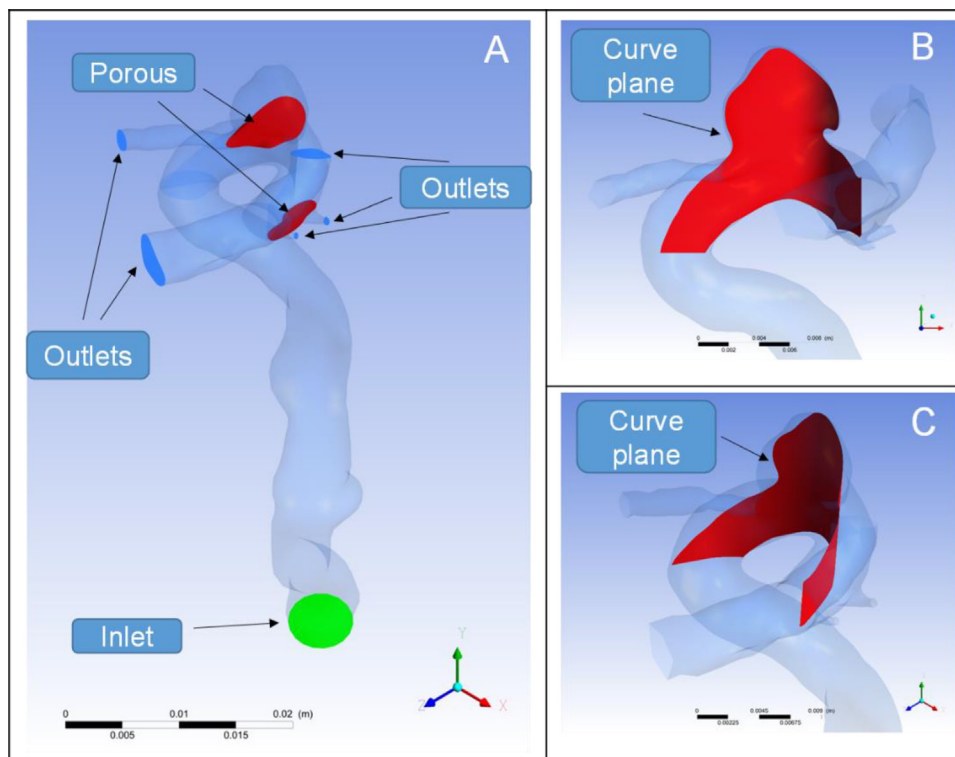

Fig. 3. The computational fluid dynamics model (A); Curve plane views in two different perspectives (B,C).

the flow analysis and the time step used in the flow analysis [21]. In the present study, LCS analyses were computed in a domain size from −0.0016 to 0.0116 mm in horizontal and from 0.00096 to 0.0114 m in vertical directions. Besides, the domain was sliced horizontally and vertically as 330 and 336 equal pieces, respectively, yielding an element size of 4E-5 m in both directions. FTLE field, drifter, and hyperbolic time calculations were evaluated for five cardiac cycles long. Furthermore, massless particles were injected into the aneurysm site to identify the number of particles staying inside the aneurysm sac to determine the warfarin's effect on hemodynamics at the aneurysm site.

While the use of anticoagulation is not a known risk factor for flow diverter failure, the primary purpose of the present study is to illustrate how aneurysm treatments with a flow diverter stent would be affected with the use of blood thinner that can reduce blood's viscosity. Therefore, blood flow with a reduced viscosity would have higher velocity than normal blood flow at the arteries. Increased blood flow at the aneurysm site can cause more mobility between the struts of the flow diverter stents and inside the aneurysm sac, delaying stagnation fluid flow formation. Besides, increased blood flow velocity can cause supraphysiological shear stress between the struts of flow diverter stents which can trigger mechanisms of delayed intracranial hemorrhages for the patient with von Willebrand Disease [35]. Due to its high potency, warfarin is commonly employed in clinical practice, especially in cases with recurrent thromboembolic events due to atrial fibrillation, deep vein thrombosis, and pulmonary embolus [10,11]. Current literature only covers the anticoagulants' perioperative effects for flow diverter treatment. However, unfortunately, some cases require long-term anticoagulant treatment. Presently, the impact of chronic warfarin use on flow diverter outcome is unknown. Our CFD analysis suggests that warfarin's effect on blood viscosity may determine flow diverter treatment outcome. Of course, more extensive clinical series are needed to validate our CFD findings.

3. Results and discussion

The first part of this section discusses the Eulerian approach findings, while the second part extensively reveals Lagrangian analysis results. Fig. 4 illustrates the key features of the former approach for normal and warfarin added blood results of aneurysm site at systole and diastole instants. Velocity contour plots given in the first row of Fig. 4 indicate that blood moves nearly 30% faster for warfarin added blood cases than normal blood flow cases. This means blood has higher kinetic energy when it enters the aneurysm sac yielding more fluid movement in the aneurysm sac. This may not be the preferred choice in the clinic since more blood flow mobility inside the sac can delay possible stagnation fluid region formations in the sac, requiring more time for occlusion.

On the other hand, the pressure contour plot shows an insignificant difference between normal, and warfarin added blood flow, implying that static pressure is dominant compared to dynamic pressure in the aneurysm region. Finally, as the blood viscosity decreases for the blood with warfarin case, the velocities in the artery increase, causing increased velocity gradients and wall shear stresses. Wall shear stress seems high at the aneurysm neck; however, it only reaches over 6 Pa at the systole instant of warfarin added blood flow case.

In the present study, the LCSs analysis provided FTLE fields, hyperbolic time (HT), and particle tracking results to precisely quantify the effect of warfarin in blood flow. Since the time evolution of FTLE and HT inside an aneurysm sac was investigated by some other studies [16,36], FTLE and HT contour plots of aneurysm site at the end of the 5th cycle are presented here in Figs. 5 and 6, respectively. Firstly, three distinct flow regions, namely jailed, unjailed, and recirculation flow regions, can be identified from FTLE contour plots of both normal blood (Fig. 5 (A)) and warfarin added blood flows (Fig. 5(B)). Secondly, decelerated blood flow creates a blocked zone named jailed flow region due to an FD placement at the aneurysm neck for normal blood (Fig. 5(A)). However, a certain amount of blood with less viscosity keeps entering inside the aneurysm, allowing unjailed flow region formation for blood with warfarin cases. Thirdly, blood entering into the aneurysm sac forms vortex regions, and the magnitude of these regions provide information about the energy level of the blood that has already entered the aneurysm sac. Therefore, larger vortex regions exist for the blood with warfarin case than normal blood case since warfarin use makes
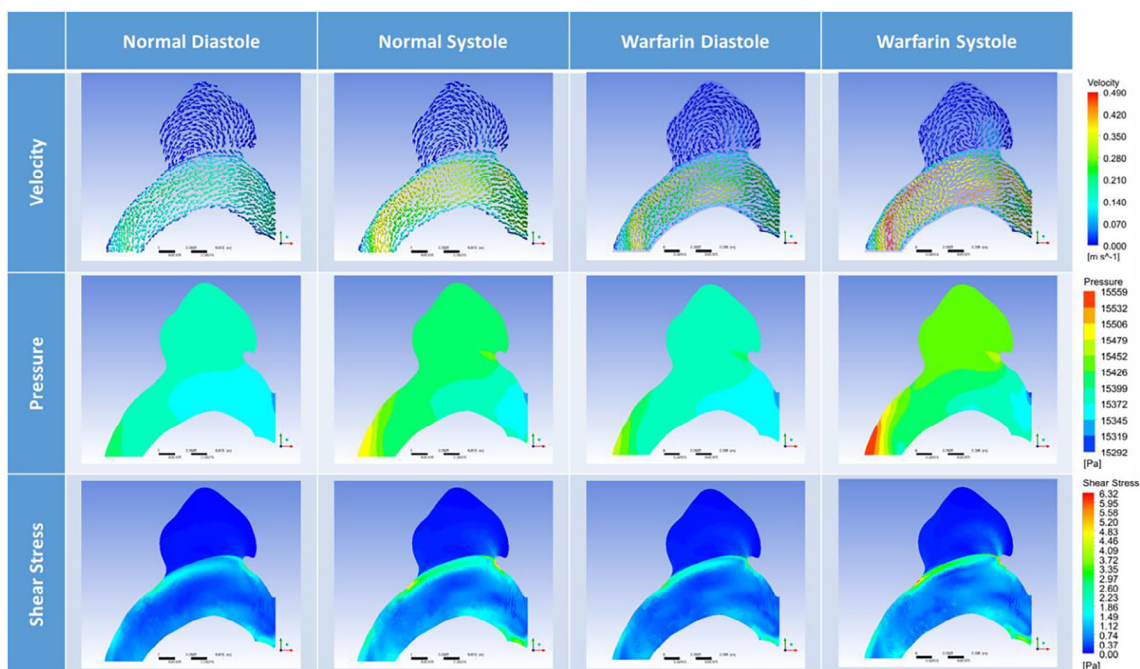

Fig. 4. Fluid velocity, pressure, and shear stress contour plots for simulation without and with warfarin at the systole and diastole instants.
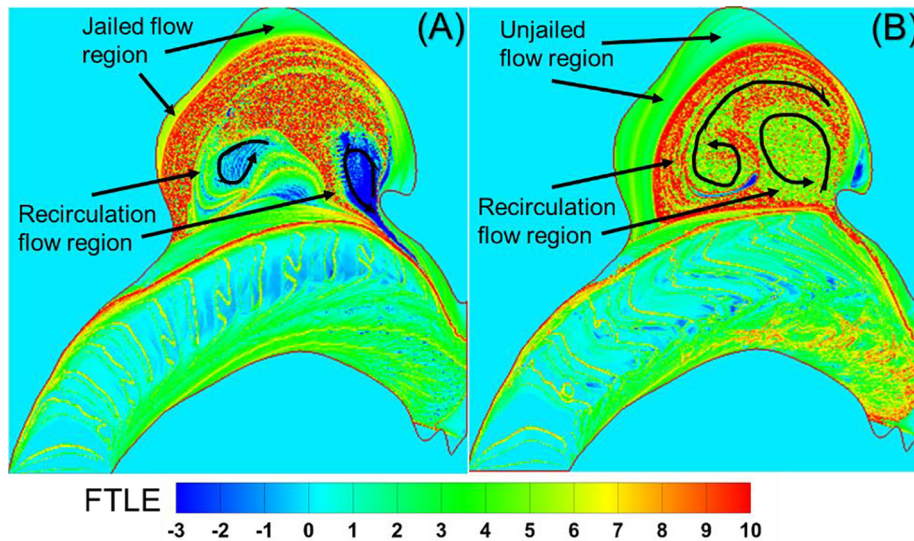
Fig. 5. Finite-time Lyapunov exponent (FTLE) fields at the aneurysm site for normal blood (A) and warfarin added blood flows (B) at the end of the 5th cardiac cycle.
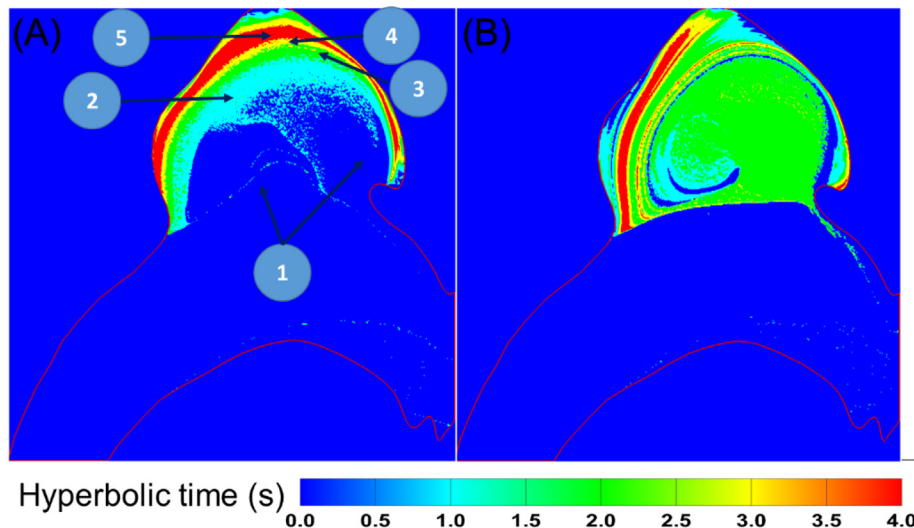

Fig. 6. Hyperbolic time contour plot at the aneurysm site for normal (A) and warfarin added blood flow (B) at the end of the 5th cardiac cycle.
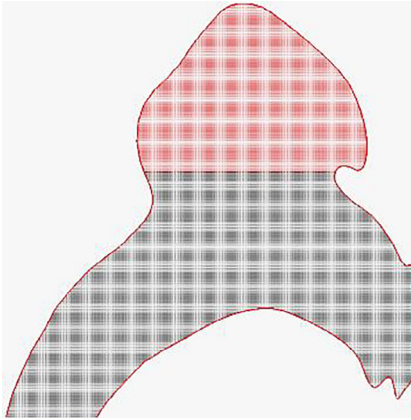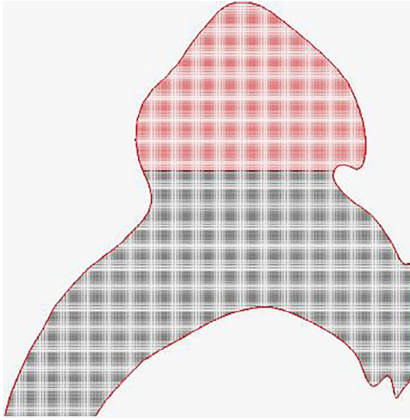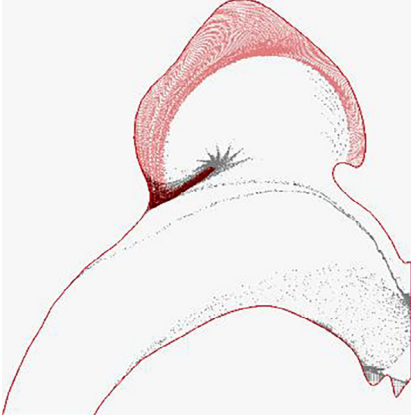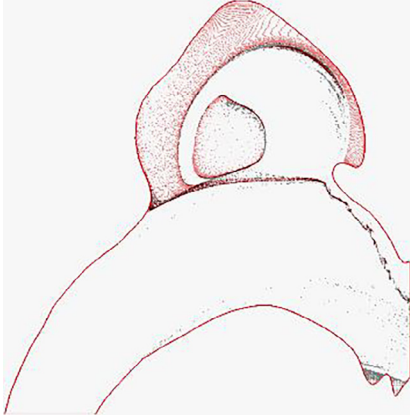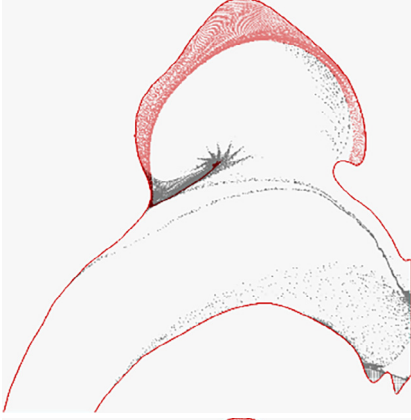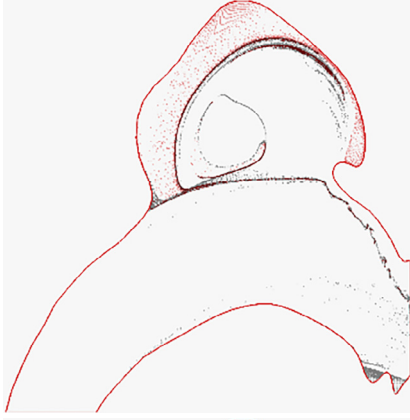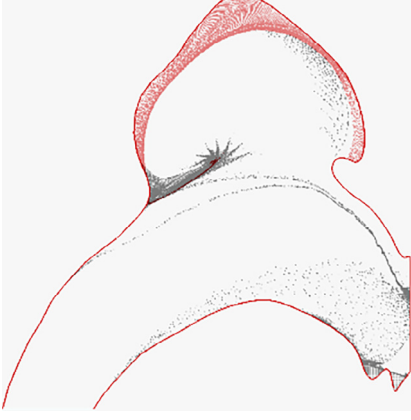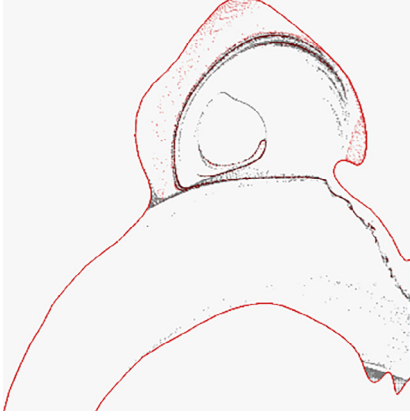
blood less viscous, allowing larger blood velocity inside the aneurysm sac.

Hyperbolic time analysis was also performed using Eulerian velocity vector data to identify the time needed to form fluid zones inside the aneurysm sac. Therefore, hyperbolic time contour plots of normal and warfarin added blood flow was represented at the aneurysm site at the end of the 5th cardiac cycle in Fig. 6. The regions in the aneurysm sac were numbered from 1 to 5 to illustrate formed fluid flow zones' shapes and the amount of time required for those zones' to occur. For example, the regions named with numbers 1, 2, 3, 4, and 5 emerge nearly at 0.5 s, 1 s, 2 s, 3 s, and 4 s, respectively, for normal blood cases as shown in Fig. 6 (A). However, blood flow entering into the aneurysm sac occupies a large portion of the sac as the green-colored region takes about 2 s for the warfarin added blood case, as given in Fig. 6(B). Therefore, blood with less resistance to flow due to low viscosity enters the sac and causes large recirculation zone formation in the aneurysm sac for warfarin added flow case.

The last part of the LCS analysis is aimed to understand the movement of fluid particles at the aneurysm site just after FD
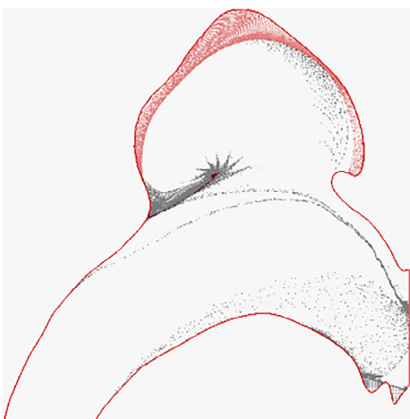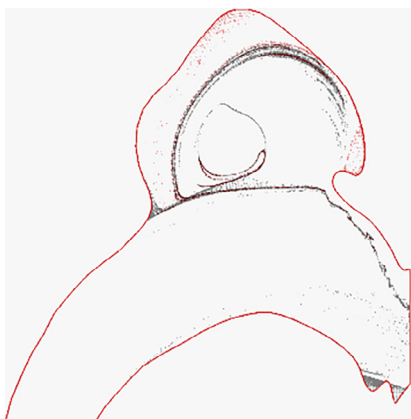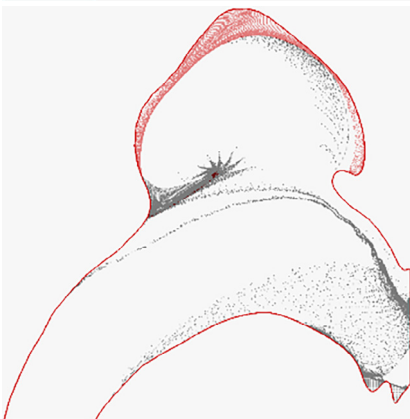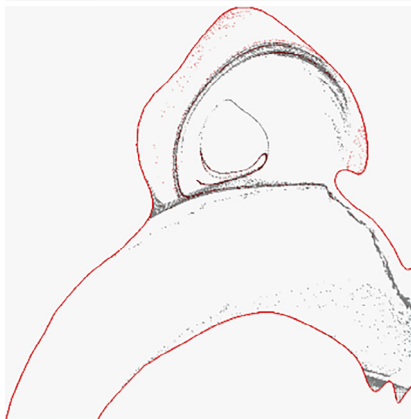
placement to the aneurysm neck. Therefore, blood initially inside the aneurysm sac and below the FD stent were marked as red and black colored fluid particles, respectively. Furthermore, nearly 25,000 black-colored particles were seeded every 1/10th of the cardiac cycle from the inlet of the numerical model to visualize hemodynamics at the aneurysm site. Table 1 shows the time evolution of fluid particles at the aneurysm site for both normal and warfarin added blood cases. There is a clear distinction between stagnated regions of normal and warfarin added blood flow results starting from the end of the first cardiac cycle. It is realized that red-colored particles representing blood initially at the aneurysm sac resists staying (i.e., jailed) near the inner wall of the aneurysm, indicating that incoming flow passing thru FD stent does not have enough kinetic energy to reach those regions. However, red-marked fluid particles of warfarin added blood cannot withstand the incoming flow and washed away from the aneurysm's inner wall even just after the 2nd cardiac cycle (i.e., 160th-time step). Therefore, the evaluation of stagnated regions based on CFD models can be incorrect if the numerical model does not account for the effect of

Table 1

Particle visualization plots of the fluid flow for normal blood and blood with warfarin case.

Timestep	Normal blood	Blood with warfarin
1st		
80th		
160th		
240th		

Table 1 (*continued*)

Timestep	Normal blood	Blood with warfarin
320th		
400th		

anticoagulants since warfarin added blood flow could show completely different hemodynamics in the aneurysm sac.

Although the time evolution of fluid particles at the aneurysm site was discussed in the previous section, the number of cumulative fluid particles inside the aneurysm was also monitored and quantified to evaluate the effect of anticoagulants in the patient-specific CFD models. Fig. 7 illustrates the number of fluid particles that remained inside the aneurysm sac at the end of each cardiac cycle, starting from the instant FD was implanted. Use of anticoagulant with blood flow yields more blood in the sac to be pushed away and only 12% of the nearly 25,000 fluid particles seeded from the inlet artery of the CFD model to stay inside the aneurysm sac. This implies that no stagnated region formation or jailed fluid par-

ticles can occur when warfarin is added into the blood flow. However, without taking account of anticoagulants, the CFD model provides over 65% of the seeded particles to reside in the sac, indicating the possibility of stagnated region formation or jailed fluid particles' existence. The deviation between two CFD models can undermine the effectiveness of patient-specific CFD models since the difference between blood and warfarin added blood flows becomes more extensive with every heartbeat.

4. Conclusion

In this study, the effect of anticoagulants, namely warfarin, on the hemodynamics of a 49-years-old female patient's cerebral aneurysm was investigated to reveal the formation of stagnated and recirculation zones in the sac. While FTLE fields illustrated stagnated or jailed particle regions and recirculation zones, hyperbolic time contours indicated the time required for these regions to form. Lastly, particle analysis was performed to determine the number of particles stays inside the aneurysm sac just after an FD implantation for both normal blood and warfarin added blood cases. Furthermore, the deviation between cumulative fluid particles in the aneurysm sac of normal blood and warfarin added blood flow becomes larger with every heartbeat reaching 2942 fluid particles out of 24,341 initially injected fluid particles resided inside the sac for warfarin added blood flow model. However, as many as 16,083 fluid particles were inside the sac for the normal blood flow model. This indicates that neuro-interventionalists and interventional radiologists relying on CFD models with no anticoagulants consideration to choose the most convenient FD for the
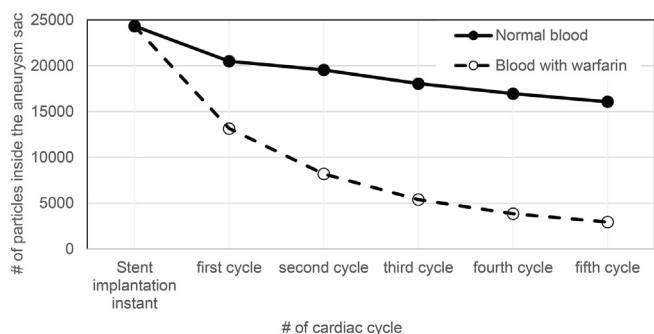

Fig. 7. Variation of the total number of particles inside the aneurysm sac for normal blood and blood with warfarin flow cases from the instant FD is placed to the end of the fifth cardiac cycle.

patient before treatment can face primarily mobile blood flow in the sac while expecting a full occlusion. Therefore, the planned recovery duration for the patient can be significantly different from the actual one, causing more visits of the patient to the hospital, which may raise concerns of FD stent choice. Hence, numerical models need to include the effect of anticoagulants in their calculations so that patient-specific model findings can match with the clinical results.

The present study can be extended by considering an anticoagulation dosage for the FD-treated patients since anticoagulation prescription in the clinic prevents platelets from clumping together to form a clot and prevent possible embolism. However, anticoagulation usage, on the other hand, causes the blood to become less viscous fluid in the arteries. Therefore, identifying the proper anticoagulant dosage has paramount importance since using a large anticoagulant dosage can yield high blood velocity at the aneurysm site, resulting in supraphysiological shear stress formation at the FD stent's struts. If a small anticoagulant dosage is used prior to FD treatment, clotting may initiate at the FD stent surfaces triggering the embolism risk. Therefore, the present study's findings can be extended to determine the proper anticoagulant dosage for patients treated with flow diverter stents.

Declaration of Competing Interest

The authors declare that they have no known competing financial interests or personal relationships that could have appeared to influence the work reported in this paper.

Acknowledgment

References

[1] Can A, Castro VM, Dligach D, Finan S, Yu S, Gainer V, et al. Elevated international normalized ratio is associated with ruptured aneurysms. Stroke 2018;49:2046–52. https://doi.org/10.1161/STROKEAHA.118.022412.

[2] Green L, Tan J, Morris JK, Alikhan R, Curry N, Everington T, et al. A three-year prospective study of the presentation and clinical outcomes of major bleeding episodes associated with oral anticoagulant use in the uk (Orange study). Haematologica 2018;103:738–45. https://doi.org/10.3324/haematol.2017.182220.

[3] Dornbos D, Katz JS, Youssef P, Powers CJ, Nimjee SM. Glycoprotein IIb/IIIa inhibitors in prevention and rescue treatment of thromboembolic complications during endovascular embolization of intracranial aneurysms. Clin Neurosurg 2018;82:268–77. https://doi.org/10.1093/neuros/nyx170.

[4] Becske T, Kallmes DF, Saatci I, McDougall CG, Szikora I, Lanzino G, et al. Pipeline for uncoilable or failed aneurysms: results from a multicenter clinical trial. Radiology 2013;267:858–68. https://doi.org/10.1148/radiol.13120099.

[5] Tadros R, Shakib S. Warfarin: Indications, risks and drug interactions. Aust Fam Physician 2010;39:476–9.

[6] Kuruvilla M, Gurk-Turner C. A review of Warfarin dosing and monitoring. Baylor Univ Med Cent Proc 2001;14:305–6. https://doi.org/10.1080/08998280.2001.11927781.

[7] Sweid A, Starke RM, Herial N, Chalouhi N, Das S, Baldassari MP, et al. Predictors of complications, functional outcome, and morbidity in a large cohort treated with flow diversion. Neurosurgery 2019:1–14. https://doi.org/10.1093/neuros/nyz508.

[8] Lee CH, Jung KH, Cho DJ, Jeong SK. Effect of warfarin versus aspirin on blood viscosity in cardioembolic stroke with atrial fibrillation: a prospective clinical trial. BMC Neurol 2019;19:1–7. https://doi.org/10.1186/s12883-019-1315-5.

[9] Oran I, Cinar C. Nöroendovasküler Girişimsel Tedavilerde anti-trombotik İlaç Kullanımı. Türk Radyoloji Semin 2018;6:11–26. https://doi.org/10.5152/trs.2018.574.

[10] Lip GYH, Banerjee A, Boriani G, Chiang Ce, Fargo R, Freedman B, et al. Antithrombotic therapy for atrial fibrillation. Chest 2018;154:1121–201. https://doi.org/10.1016/j.chest.2018.07.040.

[11] Kearon C, Akl EA, Ornelas J, Blaivas A, Jimenez D, Bounameaux H, et al. Antithrombotic therapy for VTE disease. Chest 2016;149:315–52. https://doi.org/10.1016/j.chest.2015.11.026.

[12] Yilmaz F, Gundogdu MY. A critical review on blood flow in large arteries; relevance to blood rheology, viscosity models and physiologic conditions. Kore-Australia Rheol J 2008;20:197–211.

[13] Albayrak R, Değırmencı B, Acar M, Haktanır A, Colbay M, Yaman M. Doppler sonography evaluation of flow velocity and volume of the extracranial internal carotid and vertebral arteries in healthy adults. J Clin Ultrasound 2007;35:27–33. https://doi.org/10.1002/jcu.20301.

[14] Tercanlı MF, Olcay AB, Bilgin C, Hakyemez B. Investigation of a simplified cerebral aneurysm model with non-Newtonian fluid models for three different aneurysm neck sizes using computational fluid dynamics Arcelik Company View project Hydrocyclones View project 2019.

[15] Mutlu O, Olcay AB, Bilgin C, Hakyemez B. Evaluating the effectiveness of 2 different flow diverter stents based on the stagnation region formation in an aneurysm sac using lagrangian coherent structure. World Neurosurg 2019;127:e727–37. https://doi.org/10.1016/j.wneu.2019.03.255.

[16] Mutlu O, Olcay AB, Bilgin C, Hakyemez B. Understanding the effect of effective metal surface area of flow diverter stent's on the patient-specific intracranial aneurysm numerical model using Lagrangian coherent structures. J Clin Neurosci 2020;80:298–309. https://doi.org/10.1016/j.jocn.2020.04.111.

[17] Tercanli MF, Mutlu O, Olcay AB, Bilgin C, Hakyemez B. Numerical study of a simplified cerebral aneurysm using a two different flow diverter stent modeling. TIPTEKNO 2019 - Tip Teknol Kongresi 2019. https://doi.org/10.1109/TIPTEKNO.2019.8895092.

[18] Mutlu O, Olcay AB, Bilgin C, Hakyemez B. Evaluating the effect of the number of wire of flow diverter stents on the nonstagnated region formation in an aneurysm sac using Lagrangian coherent structure and hyperbolic time analysis. World Neurosurg 2020;133:e666–82. https://doi.org/10.1016/j.wneu.2019.09.116.

[19] Olcay AB. Investigation of a wake formation for flow over a cylinder using Lagrangian coherent structures. Prog Comput Fluid Dyn An Int J 2016:126. https://doi.org/10.1504/PCFD.2016.075159.

[20] Olcay AB, Krueger PS. Measurement of ambient fluid entrainment during laminar vortex ring formation. Exp Fluids 2008;44. https://doi.org/10.1007/s00348-007-0397-9.

[21] Shadden SC, Arzani A. Lagrangian postprocessing of computational hemodynamics. Ann Biomed Eng 2015;43:41–58. https://doi.org/10.1007/s10439-014-1070-0.

[22] Shadden SC, Taylor CA. Characterization of coherent structures in the cardiovascular system. Ann Biomed Eng 2008;36:1152–62. https://doi.org/10.1007/s10439-008-9502-3.

[23] Shadden SC, Astorino M, Gerbeau J-F. Computational analysis of an aortic valve jet with Lagrangian coherent structures. Chaos 2010;20. https://doi.org/10.1063/1.3272780.

[24] Olcay AB, Amindari A, Kirkkopru K, Yalcin HC. Characterization of disturbed hemodynamics due to stenosed aortic jets with a Lagrangian Coherent structures technique. J Appl Fluid Mech 2018;11. https://doi.org/10.18869/acadpub.jafm.73.245.28185.

[25] Shadden SC, Lekien F, Marsden JE. Definition and properties of Lagrangian coherent structures from finite-time Lyapunov exponents in two-dimensional aperiodic flows. Phys D Nonlinear Phenom 2005;212:271–304. https://doi.org/10.1016/j.physd.2005.10.007.

[26] Peacock T, Haller G. Lagrangian coherent structures: the hidden skeleton of fluid flows. Phys Today 2013;66:41–7. https://doi.org/10.1063/PT.3.1886.

[27] Haller G. Distinguished material surfaces and coherent structures in three-dimensional fluid flows. Phys D Nonlinear Phenom 2001;149:248–77. https://doi.org/10.1016/S0167-2789(00)00199-8.

[28] Pierrehumbert RT. Large-scale horizontal mixing in planetary atmospheres. Phys Fluids A Fluid Dyn 1991;3:1250–60. https://doi.org/10.1063/1.858053.

[29] Green MA, Rowley CW, Smits AJ. Using hyperbolic Lagrangian coherent structures to investigate vortices in bioinspired fluid flows. Chaos 2010;20:17510. https://doi.org/10.1063/1.3270045.

[30] Mutlu O, Salman HE, Yalcin HC, Olcay AB. Fluid flow characteristics of healthy and calcified aortic valves using three-dimensional lagrangian coherent structures analysis. Fluids 2021;6:203. https://doi.org/10.3390/fluids6060203.

[31] Reza MMS, Arzani A. A critical comparison of different residence time measures in aneurysms. J Biomech 2019;88:122–9. https://doi.org/10.1016/j.jbiomech.2019.03.028.

[32] Arzani A, Gambaruto AM, Chen G, Shadden SC. Lagrangian wall shear stress structures and near-wall transport in high-Schmidt-number aneurysmal flows. J Fluid Mech 2016;790:158–72. https://doi.org/10.1017/jfm.2016.6.

[33] Arzani A, Gambaruto AM, Chen G, Shadden SC. Wall shear stress exposure time: a Lagrangian measure of near-wall stagnation and concentration in cardiovascular flows. Biomech Model Mechanobiol 2017;16:787–803. https://doi.org/10.1007/s10237-016-0853-7.

[34] Duvernois V, Marsden AL, Shadden SC. Lagrangian analysis of hemodynamics data from FSI simulation. Int J Numer Method Biomed Eng 2013;29:445–61. https://doi.org/10.1002/cnm.2523.

[35] Oran I. Flow-diverting stent and delayed intracranial bleeding: the case for discussing acquired von Willebrand disease. Platelets 2021;32:432–5. https://doi.org/10.1080/09537104.2020.1754379.

[36] Mutlu O, Olcay AB, Bilgin C, Hakyemez B. Evaluating the effects of the wire number of flow diverter stents on the non-stagnated region formation in an aneurysm sac using Lagrangian coherent structure and hyperbolic time analysis. World Neurosurg 2019. https://doi.org/10.1016/j.wneu.2019.09.116.